Editors' Suggestion

Exactly solvable percolation problems

Fabian Coupette* and Tanja Schilling
Institute of Physics, University of Freiburg, Hermann-Herder-Straße 3, 79104 Freiburg, Germany

(Received 27 November 2021; accepted 31 January 2022; published 6 April 2022)

We propose a simple percolation criterion for arbitrary percolation problems. The basic idea is to decompose the system of interest into a hierarchy of neighborhoods, such that the percolation problem can be expressed as a branching process. The criterion provides the exact percolation thresholds for a large number of exactly solved percolation problems, including random graphs, small-world networks, bond percolation on two-dimensional lattices with a triangular hypergraph, and site percolation on two-dimensional lattices with a generalized triangular hypergraph, as well as specific continuum percolation problems. The fact that the range of applicability of the criterion is so large bears the remarkable implication that all the listed problems are effectively treelike. With this in mind, we transfer the exact solutions known from duality to random lattices and site-bond percolation problems and introduce a method to generate simple planar lattices with a prescribed percolation threshold.

DOI: 10.1103/PhysRevE.105.044108

I. INTRODUCTION

Since its introduction in the late 1950s [1], the critical phenomenon of percolation has been examined extensively by both physicists (see [2] for a review) and mathematicians (see [3] for a review). Its practical relevance spans from network theory describing, e.g., the spreading of diseases [4,5] or the design of infrastructure [6] to material science, where, e.g., flow through porous media [7] and the conductivity of filler networks dispersed in insulators [8,9] are analyzed. Through the years a rich variety of theoretical tools have been developed and refined to tackle percolation in those diverse contexts, and even the problem statement itself has been modified and extended in several different ways [10,11]. In two dimensions conformal field theory [12,13] has enabled the calculation of critical exponents, and lattice duality has been used to determine the critical point of the square lattice [3,14]. Due to the advance of computer power within the last half century, numerical methods and algorithmic optimization have gained increasing attention [15–18].

In the first part of this article we introduce an alternative characterization of percolation. Then we recall exact solutions to various structurally different percolation problems and the methods originally used to solve them, and we discuss their common denominator: the treelike structure, which allows for the application of our method. Then we show that the method can be used to design networks of a prescribed percolation threshold, and we extend the spectrum of exactly solvable percolation problems.

II. MEAN FIELD PERCOLATION

The idea of the approach we present in the following is based on an alternative characterization of percolation threshold which we will first derive and then apply to the full range of exactly solved percolation problems. For the sake of readability, we initially define the required quantities only for homogeneous bond percolation in a discrete system. However, the generalization to site percolation, site-bond percolation, and also continuum problems is straightforward and will be exercised as the article progresses.

On a connected graph $G(V, E)$ with vertices V and edges E a bond percolation model is defined by assigning a probability p to each edge of being *open*. Two vertices are connected if there is an open path between them, i.e., a sequence of open edges linking one vertex to the other. (Note that in the literature the term *occupied* is often used in place of *open*, in particular, in the context of site percolation rather than bond percolation problems. The meaning of the terms is the same. Here, we follow the nomenclature of the textbook by Grimmett [3].)

The percolation probability $\Theta(p)$ is defined as the probability that an arbitrarily assigned vertex, which we call the origin $\mathcal{O}$, is part of an infinite connected component. The percolation threshold p_c demarcates the edge probability for which the percolation probability ceases to be zero,

$$\Theta(p) > 0 \quad \text{for} \quad p > p_c, \tag{1}$$

$$\Theta(p) = 0 \quad \text{for} \quad p < p_c, \tag{2}$$

formally defined by [3]

$$p_c := \sup\{p : \Theta(p) = 0\}. \tag{3}$$

For all systems we treat here, we can define a metric that characterizes the distance between two sites or particles. For $G(V, E)$ specifically we can take the number of edges visited on the shortest path between two given vertices as metric. Given a vertex A, all the edges incident to A together with the vertices linked by those edges form a subgraph we label the 1-neighborhood $\mathcal{N}_1(A)$ of A. (See the top left panel of Fig. 1 for an illustration. The 1-neighborhood of the circle with the

*fabian.coupette@physik.uni-freiburg.de

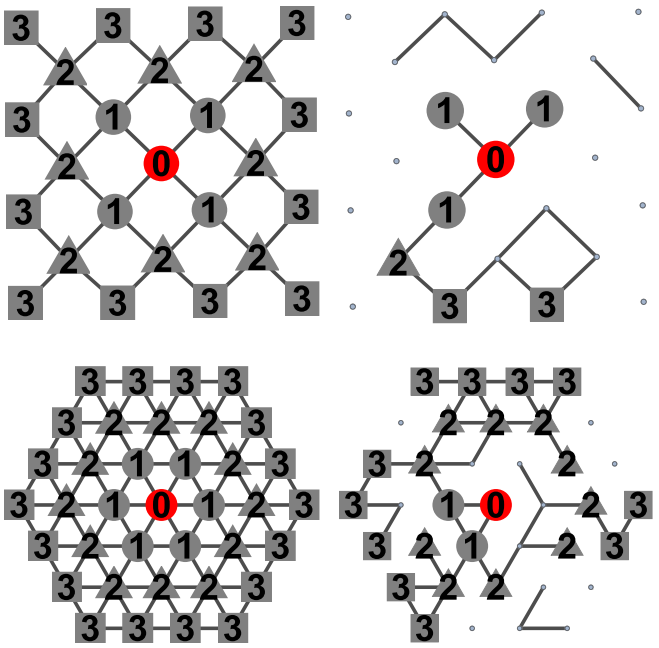

FIG. 1. Depiction of the vertex decomposition $(V_k)_{k\in\mathbb{N}}$. All panels illustrate the 3-neighborhood of the origin; the top panels show the square lattice, and the bottom panels show the triangular lattice. In the left panels all edges are drawn, while the right panels show a specific configuration of the lattice displaying only open edges. The numbers on the vertices correspond to the index k of the associated vertex set V_k. On the right only vertices contributing to the surface activity are given a number.

number 0 is formed by the circles with the number 1 and the lines connecting them to the circle with the number 0.) Recursively, we then define the k-neighborhood of a vertex A as the union of 1-neighborhoods of all vertices in the $(k-1)$-neighborhood,

$$\mathcal{N}_k(A) = \bigcup_{X\in V(\mathcal{N}_{k-1}(A))} \mathcal{N}_1(X), \tag{4}$$

where the union of graphs is simply the union of the corresponding vertex and edge sets. Specifying a vertex of the lattice as the origin $\mathcal{O}$ naturally decomposes the vertices into mutually disjoint vertex sets,

$$V_k := V(\mathcal{N}_k(\mathcal{O})) \setminus V(\mathcal{N}_{k-1}(\mathcal{O})). \tag{5}$$

That is, the vertex set V_k represents the surface of the neighborhood $\mathcal{N}_k$. With $V_0 = \{\mathcal{O}\}$ each vertex of G is uniquely sorted into one V_i. Figure 1 illustrates the topology of the vertex sets V_k for the square and triangular lattices.

If, for a given configuration of the system, there is a $\hat{k} \in \mathbb{N}$ so that none of the vertices in $V_{\hat{k}}$ are connected to the origin, the same holds by construction for any V_k with $k > \hat{k}$. As a consequence, in this case there cannot be an infinite cluster containing the origin. An infinite cluster needs to intersect each surface V_k in at least one place. Importantly, we have to specify only the degrees of freedom of the subgraph $\mathcal{N}_{\hat{k}+1}(\mathcal{O})$ to realize that the cluster around the origin is finite.

We call a vertex *active* if it is connected to the origin by a sequence of open edges. Accordingly, we define the *surface activity* $o(V_k)$ as the number of active vertices in V_k with the graph restricted to the k-neighborhood of the origin. Therefore, for a given configuration of the full graph, $o(V_k)$ comprises only those active vertices in V_k for which the connection to the origin does not rely on any vertex of V_{k+1}. (See the top right panel of Fig. 1 for an illustration. In this specific realization some of the vertices which are not labeled by numbers are connected to the origin by open bonds, but they cannot be reached from the origin by a sequence of vertices with strictly increasing label k. Hence, they do not contribute to the surface activity.)

If $\Theta(p) > 0$, with probability p, there is at least one active vertex in any V_k so that the average activity of any V_k is larger than p. Therefore,

$$\lim_{k\to\infty} \mathbb{E}[o(V_k)] \geqslant \Theta(p) > 0. \tag{6}$$

(We use the notation $\mathbb{E}$ here for the expected value rather than angle brackets, which are common in the statistical physics literature, because the angle brackets might be misunderstood as thermal expectation values. The discussion we present here is not limited to thermal ensembles.) Conversely, if the growth of the size of the vertex sets V_k is controlled $|V_k| \leqslant Ck^m$ for a fixed m, then $\Theta(p) = 0$ implies

$$\lim_{k\to\infty} \mathbb{E}[o(V_k)] = 0. \tag{7}$$

This equality is far from trivial; however, if the average surface activity is asymptotically nonzero, the mean cluster size χ is necessarily infinite. Especially in the mathematical literature (e.g., [3]), the divergence of the mean cluster size is associated with its own threshold,

$$p_T := \sup\{p : \chi(p) < \infty\}. \tag{8}$$

We now define an alternative percolation threshold,

$$p_s := \sup\{p : \lim_{k\to\infty} \mathbb{E}[o(V_k)] = 0\}, \tag{9}$$

which evidently satisfies

$$p_T \leqslant p_s \leqslant p_c. \tag{10}$$

For a square lattice of arbitrary dimension it has been shown that p_T equals p_c [3,19]. The proof relies on the controlled growth of the number of sites in a ball around the origin, which is straightforwardly generalized to more complicated finite-dimensional lattices. Thus, $p_T = p_s = p_c$ for this class of lattices; that is, our criterion will correctly reproduce the percolation threshold. General graphs require more care, but the Bethe lattice, as we will show below, is an example satisfying $p_s = p_c$ even though the surface grows exponentially with the layer. It stands to reason that a nonzero asymptotic average surface activity is, indeed, an equivalent defining characteristic of percolation for all problems we are concerned with within this article.

We can hence deduce whether the system is percolating from the average surface activity $\mathbb{E}[o(V_k)]$. Notice that $o(V_k)$ is always the activity with only $\mathcal{N}_k$ being integrated out so that the average surface activity is different from the pair connectedness analyzed in the connectedness percolation theory introduced by Coniglio *et al.* [20], as vertices in V_k that are activated through higher order neighborhoods are not taken into

account. Since all k-neighborhoods contain only finitely many degrees of freedom, there is always an active vertex in every V_k with finite probability. Clearly, the system is percolating if for some $\varepsilon > 0$

$$\exists\, K \in \mathbb{N} \;:\; \forall k > K \;\; \mathbb{E}[o(V_k)|o(V_K) = 1] \geqslant \varepsilon. \tag{11}$$

The slash in the expectation indicates the conditional average. For treelike graphs the average activity of a layer depends exclusively on the activity of the previous layer and, importantly, not on its microscopic configuration. In this case we need to describe only the transition between $o(V_{k+1})$ and $o(V_k)$ in order to estimate $\lim_{k\to\infty} \mathbb{E}[o(V_k)]$, leading to the stronger condition for percolation

$$\mathbb{E}[o(V_{k+1})|o(V_k) = 1] = 1. \tag{12}$$

In essence the above criterion demands that the system percolates if a single active vertex on the surface of the cluster containing the origin on average induces another active vertex on the subsequent surface. Equation (12) can be interpreted as a different way of writing the survival condition of a Galton-Watson branching process. Intuitively, one might expect treelike systems to be the only systems for which the above criterion yields the correct critical parameters as loops would cause correlations disturbing the artificial hierarchy. The central insight of this article is that there are more treelike systems than one might think. But before we show this we briefly describe percolation on a tree with our formalism.

A. Bethe lattice

We assign the origin to an arbitrary vertex. Then $\mathcal{O}$ has z neighbors, with z being the coordination number. Each vertex in V_k, however, has $z-1$ neighbors in V_{k+1} for $k = 1, 2, \ldots$. The average number of active nodes in V_k can be expressed in a simple recurrence. Every active node in V_k induces $(z-1)p$ active nodes in V_{k+1}. Thus,

$$\mathbb{E}[o(V_{k+1})] = (z-1)p\, o(V_k). \tag{13}$$

Averaging on both sides yields

$$\mathbb{E}[o(V_{k+1})] = (z-1)p\, \mathbb{E}[o(V_k)]. \tag{14}$$

In combination with $\mathbb{E}[o(V_1)] = zp$, the explicit average activity is apparently

$$\mathbb{E}[o(V_k)] = zp((z-1)p)^{k-1}. \tag{15}$$

Accordingly, the asymptotic activity is given by

$$\lim_{k\to\infty} \mathbb{E}[o(V_k)] = \begin{cases} 0 & p < \frac{1}{z-1}, \\ \frac{z}{z-1} & p = \frac{1}{z-1}, \\ \infty & p > \frac{1}{z-1}. \end{cases} \tag{16}$$

That is, we find the percolation threshold at $p_c = \frac{1}{z-1}$, as expected. In the original derivation of this result [21] generating functions were used. However, in the same publication the idea that a vertex needs, on average, one neighbor for a "cascade process" to build an infinite cluster is mentioned as a plausibility check.

This reasoning can be applied to any system with a self-similar structure because the average activity depends only on the average activity on the previous layer. Therefore, we can coarse grain the entire subgraph $\mathcal{N}_k(\mathcal{O})$ into one number—the average cluster surface activity. The map

$$\mathbb{E}[o(V_k)] \mapsto \mathbb{E}[o(V_{k+1})], \quad x \mapsto (z-1)px, \tag{17}$$

can hence be interpreted as a renormalization transformation with the cluster surface activity $o(V_k)$ as the scaling variable that becomes marginal at the percolation threshold. For the regular Bethe lattice this map is particularly simple, but the model can be extended to different degree distributions and probability distributions; the critical manifold is always given by a variation of condition (12). As an immediate consequence, we recover, for instance, the strict lower bound of long range percolation in one dimension [22] because we can construct a Bethe lattice containing that problem as a subgraph. Random graphs provide another example of systems that require a little effort to discover their tree nature.

B. Random graphs

We consider the Erdős-Rényi $G(N, p)$ model, i.e., unlabeled graphs with N nodes and a constant probability $p = 1 - q$ for an edge between any two nodes to be open. In the initial publication [23], Erdős and Rényi already discussed a variety of properties, including the emergence of a giant component if $Np = 1$, containing $\mathcal{O}(n^{\frac{2}{3}})$ nodes almost surely in the thermodynamic limit $N \to \infty$. For $Np = 1 + \epsilon$ with an arbitrarily small positive ϵ, a positive fraction of nodes is part of the giant component, so as N goes to infinity, the graph contains an infinite cluster almost surely, i.e., $Np_c \leqslant 1$. Conversely, for $Np = 1 - \epsilon$ the cluster size distribution decays at least exponentially fast, so that the mean cluster size remains finite almost surely, $Np_T \geqslant 1$, and with Eq. (10) $Np_T = Np_s = Np_c = 1$. We will show that random graphs in the thermodynamic limit are effectively trees when it comes to percolation.

We again declare an arbitrary node the origin; however, the vertex sets $(V_k)_{k>0}$ need to be defined differently as the 1-neighborhood of the origin already contains all vertices of $G(N, p)$. The activity of V_1 is distributed according to the binomial distribution $B(N-1, p)$, so that the average activity is simply

$$\mathbb{E}[o(V_1)] = (N-1)p. \tag{18}$$

If we now demand $\mathbb{E}[o(V_1)] = 1$, we effectively treat the system as a Bethe lattice with coordination number N. Interestingly, we obtain the correct percolation threshold in the limit $N \to \infty$, already indicating that clusters on $G(N, p)$ remain treelike in the subcritical regime. For a given configuration of the 1-neighborhood $\mathcal{N}_1(\mathcal{O})$, we can coarse grain all active vertices of V_1 into a new macrovertex $\mathcal{O}'$. Since each of the coarse-grained vertices has an individual potential connection to each vertex in the remainder of the graph, $\mathcal{O}'$ is connected to any other vertex in the graph through a k-multiedge. As a connection requires only one of these k edges to be open, the multiedge can be interpreted as single edge with probability $p' = 1 - q^k$. We define $o(V_2)$ as the number of active neighbors of the macrovertex $\mathcal{O}'$. Continuing this procedure indefinitely gives rise to a stochastic process,

$$X_{n+1} = \xi_n(X_n), \tag{19}$$

with $X_0 = 1$, where $\xi_n(X_n)$ is a random variable drawn from the binomial distribution

$$B\left(N - \sum_{i=0}^{n} X_i,\, 1 - q^{X_n}\right). \tag{20}$$

Each trajectory of this process is a sequence of surface activities $(o(V_1), o(V_2), \dots)$, so that the average surface activity $\mathbb{E}[o(V_k)]$ is well defined as the average value of X_k. Accordingly, we can solve the percolation problem by studying the limit of the sequence $(\mathbb{E}[X_k])_{k\in\mathbb{N}}$. In the thermodynamic limit either the sum $\sum_{i=0}^{n} X_i$ is small compared to N, or the cluster containing the origin already encompasses a positive fraction of the system corresponding to percolation. Hence, the simplification $N - \sum_{i=0}^{n} X_i \approx N$ is well controlled in the subcritical regime. The simplified stochastic process is Markovian, and we swiftly find for $Np = 1 - \varepsilon$

$$\begin{aligned}\mathbb{E}[X_{n+1}] &= \sum_{j=0}^{N} N\,(1-q^j)\mathbb{P}(X_n = j)\\ &= \sum_{j=0}^{N} N\left[1 - \left(1 - \frac{1-\varepsilon}{N}\right)^j\right]\mathbb{P}(X_n = j)\\ &< \sum_{j=0}^{N}(1-\varepsilon)\; j\;\mathbb{P}(X_n = j) = (1-\varepsilon)\mathbb{E}[X_n], \end{aligned}\tag{21}$$

which implies $\lim_{k\to\infty}\mathbb{E}[o(V_k)] = 0$. The $\mathbb{P}$ denotes the probability of the event given as argument. Conversely, for $Np = 1 + \varepsilon$ we can use the same reasoning to show that if $X_n < \frac{2\varepsilon}{(1+\varepsilon)^2} =: P_\varepsilon$, the expectation $\mathbb{E}[X_{n+1}] > X_n$, which requires the process to reach P_ε, i.e., a finite fraction of the vertices of the system, with finite probability. In sum we obtain $p_s = 1$ as expected.

This analysis of percolation on Erdős-Rényi random graphs illustrates how percolation on graphs containing loops can still be mapped onto a branching process and analyzed in the corresponding framework.

Small world networks provide a generalization of this model which also allows for an exact solution and can be treated in a similar way [4]. The local clusters of a small world network can each be coarse grained into a single vertex of a random graph. The connection probability between two vertices in the random graph depends on the sizes of the corresponding coarse-grained clusters. As all the local clusters are finite, percolation requires a giant component of connected coarse-grained clusters in the thermodynamic limit. This implies that a vertex of the coarse-grained graph has to have at least one neighbor on average, resulting again in the exact threshold.

Notice that coarse graining an ensemble of graph configurations into an averaged observable is inherently a mean field approach. Correlations between different layers of the construction are neglected. For random graphs we can get away with that because in the thermodynamic limit the probability of revisiting a vertex in the hierarchic formation of the percolating cluster is negligible. A critical graph is essentially a forest of trees; that is, the number of vertices contained in tree components is $N + \mathcal{O}(1)$ [24]. Naturally, we would expect the method to fail once the graph topology imposes correlations, and the clusters would contain cycles. Nevertheless, the same mean field approach also provides all exact bond percolation thresholds on two-dimensional (2D) lattices, as we are going to demonstrate in the next section.

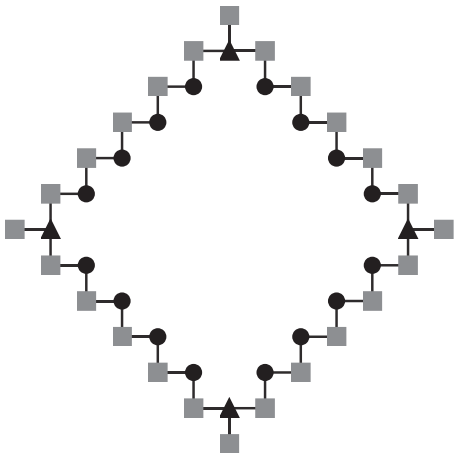

FIG. 2. The transition from V_k (circles and triangles) to V_{k+1} (squares) on the square lattice. There are two different types of local environments depicted by different shapes: Circles have two shared neighbors on the subsequent layer, while triangles have an additional exclusive neighbor.

C. Percolation on 2D lattices

Much work has been and still is dedicated to the percolation problem on planar lattices. In contrast to higher-dimensional problems the topology of the plane provides a rigorous characterization of the critical manifold by use of the dual lattice (bond percolation) or the matching lattice (site percolation). In recent years, the usage of this additional bit of information has become more and more refined, resulting in a couple of exact solutions [25–28] as well as new approximation or simulation techniques [18,29,30] which allow for extremely precise determination of percolation thresholds on general planar lattices. We do not want to engage in this pursuit for precision but rather provide a different perspective upon the problems which have been solved exactly.

Historically, the solution of bond percolation on the square lattice was, at least to mathematicians, the first "milestone" towards today's understanding of 2D lattice percolation. Following this protocol, we motivate our approach by analyzing the square lattice first.

1. Bond percolation on the square lattice

All vertices on the square lattice are equivalent. Thus, we chose an arbitrary vertex as the origin and, in complete analogy to the previous analysis of random graphs, construct the hierarchy of neighborhoods with corresponding mutually exclusive vertex sets $(V_k)_{k\in\mathbb{N}}$. The topology of these vertex sets is illustrated in Fig. 2. For each k there are two types of local environments (circles and triangles), but as k grows large, the contribution of the "triangle environment" will become negligible. Thus, asymptotically, each node in V_k has two potential neighbors in V_{k+1}, and "adjacent" nodes in V_k have a common potential neighbor. Percolation requires the

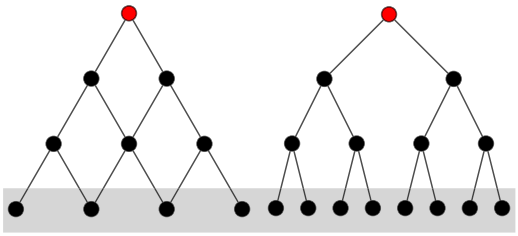

FIG. 3. Left: Asymptotic substitute lattice for the square lattice. Right: Bethe lattice with identical average surface (gray shading) activity at the percolation threshold.

average activity in the infinite annulus to be bounded away from zero. This property trivially applies for all finite annuli V_k as the event of an activity depends only on finitely many degrees of freedom. So we can always assume the existence of an active vertex in V_k which becomes the starting point of our analysis. We can now construct the hierarchic substitute lattice $Q \subset \mathbb{Z}^2$ depicted in Fig. 3 based on this asymptotic neighbor relationship where

$$Q = \{(m, n) \in \mathbb{Z}^2 \mid m, n \geqslant 0\}. \tag{22}$$

Clearly, this sublattice corresponds to a quadrant of the square lattice. For this sublattice, it was shown that the critical parameters coincide with those of the half plane [31], and the equality of the percolation threshold to the complete lattice has been conjectured but has yet to be shown. In what follows, we provide a potential first step towards proving this conjecture by providing evidence that on Q the mean cluster size of the component containing the origin diverges at $p = \frac{1}{2}$. Q inherits the hierarchic decomposition of $\mathbb{Z}^2$ via

$$V_k' = Q \cap V_k. \tag{23}$$

As for the Bethe lattice we suggest that percolation requires an active node to, on average, induce at least one of its neighbors on the subsequent layer to be active as well. Importantly, this is independent of all layers prior to the chosen vertex; that is, we neglect in-layer correlations. The average activity of V_1' is swiftly computed, resulting in

$$\mathbb{E}[o(V_1')] = 2p^2 + 2p(1-p) = 1, \tag{24}$$

which has the unique solution $p = \frac{1}{2}$ in the interval [0,1]; that is, we obtain the correct percolation threshold for the square lattice.

$p = \frac{1}{2}$ is also the percolation threshold of the Bethe lattice with coordination number $z = 3$. Indeed, powers of the polynomial in (24) correspond to the average activity of higher layers of a symmetric tree with two branches emanating from each vertex (see Fig. 3). However, the partial lattices

$$Q_k = \{(m, n) \in Q \mid m + n \leqslant k\} \tag{25}$$

for $k > 1$ contain loops, so we cannot extrapolate in the same way for the square lattice. Yet, surprisingly, the sequence of lattices Q_k' seems to have a most remarkable property:

$$p = \tfrac{1}{2} \;\Rightarrow\; \mathbb{E}[o(V_k')] = 1 \;\forall\, k \in \mathbb{N}. \tag{26}$$

Proving this property proved cumbersome as paths can contain "upward" passages (i.e., passages which return towards the origin), which do not allow for a straightforward proof by induction. Thus, here we refer to only the analytic expressions of $\mathbb{E}[o(V_k')]$ for $k \leqslant 5$ and Monte Carlo simulations of $\mathbb{E}[o(V_k')]$ for k as large as 1000 (see Fig. 4), all being consistent with (26), which we shall treat as a combinatorial curiosity. Thus, at the critical point, $\mathbb{E}[o(V_k')] = \mathbb{E}[o(V_1')]^k = 1$, so the square lattice behaves like the Bethe lattice, despite manifestly containing loops. Naturally, the polynomials characterizing the average activity in each layer have nothing to do with their counterpart for the Bethe lattice except for their value at the critical point. At the critical point the loss in average activity due to loop formation on the square lattice is exactly canceled by the additional paths between different branches of the associated Bethe lattice. Figure 5 illustrates that relationship. As each configuration is equally likely at $p = q = \frac{1}{2}$, the sum of the number of paths connecting the root node to any of its leaf nodes in V_k is 2^k. In this sense, the square lattice acts as a tree, and hence, the percolation threshold depends only on the transition to the next layer which is governed by the single unit cell. Akin to percolation on the Bethe lattice, the edge probabilities can be different from one another and even correlated to each other; the critical manifold still satisfies

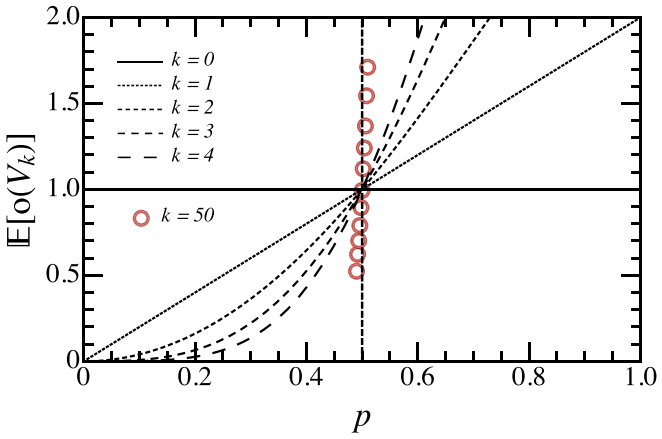

FIG. 4. The average activity of the kth layer of the asymptotic substitute of the square lattice. Lines represent analytic results, while the symbols are simulation results.

$$\mathbb{E}[o(V_1')] = 2\mathbb{P}(o(V_1') = 2) + \mathbb{P}(o(V_2') = 1) = 1. \tag{27}$$

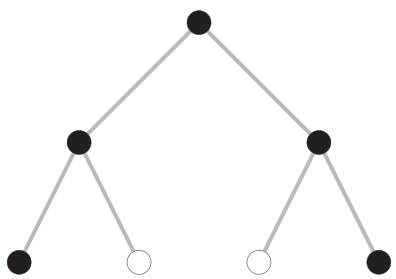

FIG. 5. Q_1 with the square lattice unit cell attached to each vertex in V_1'. In order to recover Q_2 the white vertices have to be contracted. The sum of paths connecting the root node to each of the leaf nodes individually is invariant under this vertex contraction.

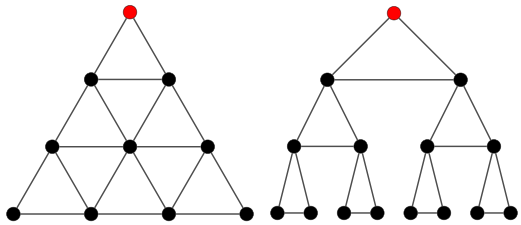

FIG. 6. Left: Asymptotic substitute lattice for the triangular lattice. Right: Triangular tree lattice; its percolation threshold corresponds to a correlated triangular lattice.

Notice that also the average surface activity is exactly conserved at the percolation threshold if the connection probabilities of the two edges in the unit cell are different. Therefore, each loop is countered by a "horizontal transfer" with the same number of open edges of each type. However, this relationship breaks down once the two leaf nodes of the unit cell can be connected by paths that do not pass the root node as, for instance, in the triangular lattice.

2. Bond percolation on triangular-type lattices

As the three terminal vertices of the triangular unit cell are equivalent, the connection probabilities have to enter symmetrically in an expression describing the percolation properties of the entire lattice. Yet if we consider the average surface activity in the above construction of the asymptotic substitute of the square lattice with added horizontal bonds between vertices on the same layer (see Fig. 6), the assignment of the root vertex artificially breaks this symmetry. The percolation threshold of the triangular tree lattice, i.e., the straightforward analog to our treatment of the square lattice depicted on the right-hand side of Fig. 6, can easily be computed following our consideration of the Bethe lattice. Denoting the three individual edge probabilities of the triangular unit cell by p_1, p_2, and p_3, with the latter one not being connected to the root node, the critical manifold reads

$$p_1 + p_2 + p_1p_3 + p_2p_3 - 2p_1p_2p_3 = 1. \tag{28}$$

In the homogeneous case $p_i = p$ the percolation threshold is roughly $p_c \approx 0.403$, which is the percolation threshold of the triangular lattice where edge 3 cannot be open without one of the other bonds being open as well. Since the configuration with only edge 3 present does not contribute to $\mathbb{E}(o(V_1'))$ the corresponding mean field prediction does not account for any system configurations featuring unit cells in this macrostate. Instead, we have again computed the percolation threshold for a square lattice with the probabilities $\mathbb{P}(o(V_1') = 1)$ and $\mathbb{P}(o(V_1') = 2)$ being only slightly varied.

Clearly, the critical manifold of the triangular lattice should be symmetric in p_1, p_2, and p_3. Moreover, if one of these probabilities vanishes, the critical manifold should reduce to the one corresponding to the square lattice. There is only one polynomial linear in all edge probabilities that meets these constraints:

$$p_1 + p_2 + p_3 + p_1p_3 + p_2p_3 + p_1p_2 - 2p_1p_2p_3 = 1, \tag{29}$$

which provides the correct critical manifold of the triangular lattice. Formally, this line of argumentation is known as the contraction-deletion method [18,32]: Starting from the most general polynomial linear in all edge probabilities

$$f(p_1, p_2, p_3) = \sum_{i,j,k\in\{0,1\}} a_{ijk}\left(p_1^{1-k}\right)q_1^k\left(p_2^{1-k}\right)q_2^k\left(p_3^{1-k}\right)q_3^k, \tag{30}$$

where $f(p_1, p_2, p_3)$ has eight parameters (each configuration initially has its own weight a_{ijk}), we use symmetry in all three arguments, reducing the number of parameters to four, and demand that we recover the solution of the square lattice when one of the arguments vanishes. This uniquely defines all remaining parameters except for a_{111}, corresponding to the configuration with all bonds open. However, this configuration is equivalent to configurations with only two edges present because the missing bond connects two vertices that are already in the same cluster. So the parameters associated with both configurations are equal. The resulting polynomial describes the maximum number of leaf nodes connected to a root node in the unit cell given that any node is a root and a leaf at the same time averaged over all configurations of the unit cell. This symmetrized surface activity provides the exact percolation threshold for the triangular lattice as the solution of

$$f(p_1, p_2, p_3) = 1, \tag{31}$$

which coincides with Eq. (29).

For any three-terminal with terminal nodes A, B, and C, f is always obtained from $\mathbb{E}[o(V_1)]$ by adding the probability of the two leaf nodes, say, B and C, being in a cluster without the root node, say, A, resulting in the simple criterion

$$f(\boldsymbol{p}_c) = 2\mathbb{P}_{\boldsymbol{p}_c}(A, B, C) + \mathbb{P}_{\boldsymbol{p}_c}(A, B, \overline{C}) + \mathbb{P}_{\boldsymbol{p}_c}(A, \overline{B}, C) + \mathbb{P}_{\boldsymbol{p}_c}(\overline{A}, B, C) = 1, \tag{32}$$

where $\boldsymbol{p}_c$ comprises the critical manifold and $P_{\boldsymbol{p}}(A, B, \overline{C})$ is the probability that A and B are in a cluster without C. Hence, the system is percolating if, on average, two terminals of a unit cell are connected to each other. This is equivalent to the criterion derived from duality, which is readily obtained from Eq. (32) by using the normalization of P, leading to

$$\mathbb{P}_{\boldsymbol{p}_c}(A, B, C) - \mathbb{P}_{\boldsymbol{p}_c}(\overline{A}, \overline{B}, \overline{C}) = 0. \tag{33}$$

Hence, Eq. (32) provides the exact bond percolation thresholds for all lattices created from a triangular hypergraph by use of the generalized star-triangle transformation [25,26,28,32–34]. Notice that we do not provide an independent proof that these percolation thresholds are exact but rather acknowledge that all exactly known percolation thresholds satisfy the criterion (32). As all these solutions depend only on an average over a microscopic fragment of the lattice, correlations between adjacent unit cells, i.e., different layers, necessarily average out. In that sense the square lattice effectively does not contain any loops, which is the consequence of the additional structure provided by duality.

The decorrelation of unit cells has a couple of interesting implications. For example, the vertex degree and the edge probabilities of the Bethe lattice, the generator, i.e., the specific unit cell embedded in a triangular hypergraph, can be entirely arbitrary and does not even have to be unique throughout the lattice as long as the unit cells are drawn randomly

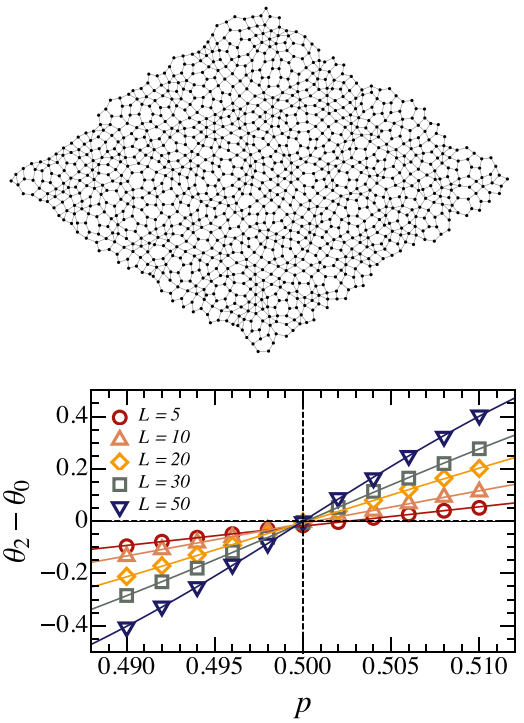

FIG. 7. Top: A pseudorandom network created from a triangular hypergraph filled with unit cells of square, triangular, and hexagonal lattices with equal probability. Bottom: Simulation results for lattices of the kind above with periodic boundary conditions sampling the graph polynomial, with Θ_2 and Θ_0 being the probabilities of obtaining a two-dimensional wrapping cluster or no wrapping cluster, respectively.

from a common distribution. This is an important generalization of the class of exactly solvable percolation problems, as it allows us to determine the percolation threshold of random networks. Figure 7 displays an instance of a pseudorandom network constructed of triangular, square, and hexagonal unit cells. The microscopic arrangement of the individual pieces is irrelevant as long as it is not correlated. In the decorrelated case the lattice can be interpreted as being created by only a single generator comprising all connection probabilities between the terminal vertices. The symmetrized average activity is straightforwardly computed as a linear combination of the polynomials describing the different unit cells. The critical values derived from the composite polynomial describe an ensemble of lattices which is dominated by the maximum entropy states. So if you pick a random infinite representative of this ensemble, its percolation threshold is equal to the ensemble average. It does even allow us to design lattices with a prescribed percolation threshold built from simple building blocks. The quasirandom lattice in Fig. 7, for example, contains triangular, square, and hexagonal unit cells with equal frequency. The linear combination of their symmetrized surface activity results in the percolation threshold $p_c = \frac{1}{2}$, in perfect agreement with the simulation results. Varying the relative frequency of the unit cells allows for an adjustment of the percolation threshold to any value between the minimum and maximum thresholds achievable with only one cell type. As the unit cells can, in principle, be arbitrarily connective or

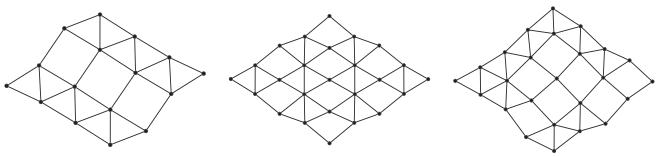

FIG. 8. Snippets of lattices created from triangular and square unit cells in equal proportion: elongated triangular lattice, $p_c \approx 0.4196$ (nonexact; left), bow-tie lattice, $p_c \approx 0.4045$ (exact; middle), and random alignment, $p_c = \sqrt{2} - 1 \approx 0.4142$ (exact; right).

scarce, this method admits the construction of a planar lattice with a prescribed homogeneous bond percolation threshold $p_c \in (0, 1)$. As long as the distribution of unit cells is uncorrelated, the mean field theory remains exact.

The impact of correlations between the types of unit cells is displayed in a comparison of different lattices generated from the same set of unit cells (see Fig. 8). The long range periodicity causes small deviations, but the mean field prediction remains fairly accurate. In that sense, an analysis of the distribution of unit cells can provide a simple mean field guess to a given network. For instance, the snub square lattice is built from the same number of triangles and squares as the lattices depicted in Fig. 8 but is not arranged according to the triangular hypergraph. Regardless, the percolation threshold $p_c \approx 0.4141$ (nonexact) is very well approximated by the mean field prediction. Curiously, we would expect the approximation to become even better once random defects destroy the long range periodicity of the lattice.

Since the generator is arbitrary, the lattice likewise does not have to be planar anymore as long as it is built from a self-dual hypergraph. The prime examples of nonplanarity and their corresponding percolation thresholds are depicted in Fig. 9. We can even decorate each individual cell with an Erdős-Rényi random graph $G(N, p)$, with N and p drawn from an arbitrary distribution, and the percolation threshold can be computed exactly in the aforementioned way.

We proceed by transferring the treelikeness to site percolation problems.

3. Site percolation

For site percolation two vertices linked by an edge are considered connected when both vertices are *open*. Accordingly, probabilities to be open are assigned to vertices rather than edges. A vertex A is active if it is open and there is a sequence of mutually adjacent open vertices linking A to the

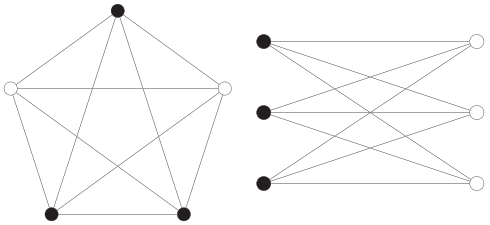

FIG. 9. Nonplanar unit cells embedded in the triangular hypergraph at the black vertices are exactly solvable: K_5: $p_c \approx 0.2528$; $K_{3,3}$: $p_c \approx 0.3903$.

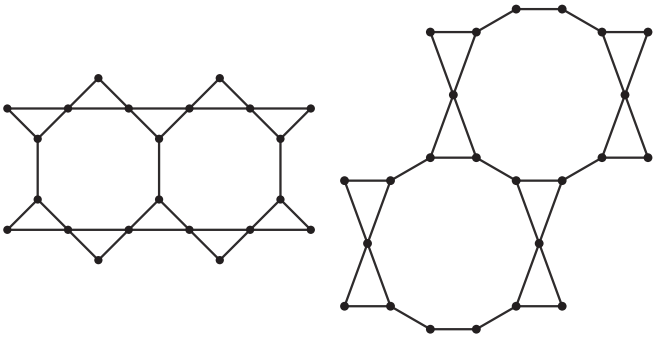

FIG. 10. Our exactly solvable site percolation problems. Left: Elongated kagome, $p^2 + 2p^3 - p^4 = 1 \rightarrow p_c \approx 0.7213$. Right: Clinched 3-12, $2p^3 + p^4 - p^5 = 1 \rightarrow p_c \approx 0.7717$.

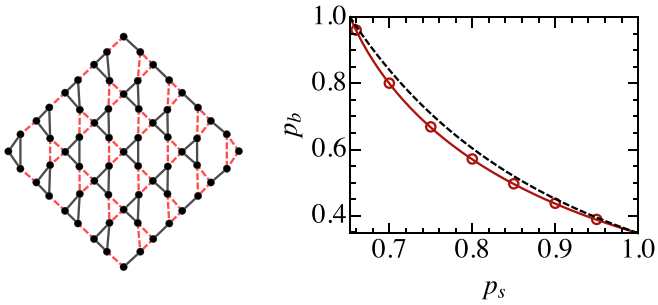

FIG. 11. Left: Kagome lattice with fixed edges (dashed red lines). Right: Critical manifold for site-bond percolation for the lattice on the left. Symbols denote simulation results, the solid line represents solutions to Eq. (34), and the dashed line is an approximation due to [36].

origin. Thus, each active vertex is open but not the other way around. Each bond percolation problem can be transformed into a site percolation problem by placing a site on each bond and connecting them if the underlying bond share a common vertex, i.e., constructing the covering lattice. So each exactly solved bond problem automatically provides the solution to a site problem (Fig. 10). The prime example is the equivalence of bond percolation on the hexagonal lattice and site percolation on the kagome lattice first acknowledged in [33]. In the previous section we obtained exact percolation thresholds due to decorrelation of unit cells. For bond percolation the fact that two unit cells share a vertex does not induce correlation between the unit cells. For site percolation, in analogy, we have to separate unit cells by bonds. For all representatives of the triangular hypergraph this means we have to replace each terminal (which is part of three unit cells at once) by a triangle formed by the three individual terminals of the corresponding unit cells. This *site-to-bond transformation* was applied by Scullard [25] to obtain the exact thresholds for the Martini lattices. However, the Martini lattices are exactly solvable as bond problems as well so that we can reiterate the transformation obtaining the lattices depicted in Fig. 10 which extend the set of exactly solvable site percolation problems. With the exception of the class of fully triangulated lattices, all known exactly solvable site percolation problems can be associated with an exactly solvable bond problem in this way. Table I lists the correspondence between solvable bond problems and the *lifted lattice* of the induced site solution. In this way any of the above exact solutions for bond percolation translates to exact solutions for site percolation on a modified lattice. The generalizations in the previous sections can also be transferred to the site percolation problem so that arbitrary probability distributions are treatable and the assignment of unit cells may be randomized.

TABLE I. The bond percolation problems in the left column correspond to site percolation problems on a *lifted* lattice. If you apply Eq. (32) to the unit cell of the lattice in the left column with sites instead of bonds being the degree of freedom, you obtain the critical polynomial for site percolation of the lattice in the right column.

Bond problem	Site problem
Triangular	Kagome
Triangular with one fixed bond	Martini B
Triangular with two fixed bonds	Triangular
Square	Martini A
Hexagonal	Martini
Martini	3-12
Martini A	Clinched 3-12
Martini B	Elongated kagome

The connection between site percolation and bond percolation puts us in a position to find specific exact solutions for site-bond percolation as well. We refer to site-bond percolation as the model for which sites and bonds are independently assigned probabilities to be open and a direct connection between two sites is established only if both sites and the bond between them are open. The key is the simultaneous decoupling of the bond and site degrees of freedom for the same unit cell. This can be realized, for example, for the kagome lattice by fixing the bond probabilities of each triangle pointing to the right to 1 (Fig. 11). The remaining edges and all vertex degrees of freedom are now decoupled from the neighboring unit cells, and we can compute the critical manifold by computing connection probabilities in a single triangular unit cell. For homogeneous bond probabilities p_b and site probabilities p_s we find the critical manifold as

$$p_s^3\left(3p_b - p_b^3\right) + 3p_s^2(1 - p_s)p_b = 1. \tag{34}$$

As expected, this result interpolates between the percolation threshold of the triangular lattice for $p_s = 1$ and the site percolation threshold of the kagome lattice for $p_b = 1$ and is in perfect agreement with the simulation results (Fig. 11). Since the precise shape of the three-terminal in between the fixed triangles is entirely arbitrary, our perspective provides an entire class of exactly solvable site-bond percolation problems.

Indeed, the only exact solution to a site-bond model on a two-dimensional lattice that we know of [35] features the other option of achieving decorrelation between unit cells, that is, fixing the terminal sites of the unit cell. If the terminals are fixed as open, the degrees of freedom of neighboring unit cells are again independent. Clearly, the sites enclosed in the unit cell just modify the connection probabilities between the terminals in the same way that bonds do. Thus, we can make straightforward use of Eq. (32) to compute the critical manifold of site-bond percolation on the hexagonal lattice with

every second site being fixed; the critical manifold is

$$p_s\left[2p_b^3 + 3p_b^2(1-p_b)\right] = p_s\left(3p_b^2 - p_b^3\right) = 1. \tag{35}$$

The same result was obtained by Kondor [35] using duality between this lattice and bond percolation on a triangular lattice with added three-site bonds. Clearly, this result is again just a representative for an entire class of exactly solvable percolation problems because every lattice with a triangular hypergraph can be lifted to an exactly solvable site-bond percolation problem by fixing only the terminal sites.

Since there are no exact solutions for three-dimensional lattices, we finally have a look at the continuum.

III. CONTINUUM PERCOLATION

In continuum percolation, site positions are continuously distributed, not necessarily homogeneously, in $\mathbb{R}^d$ and connected according to a connectivity criterion which depends on only the microscopic degrees of freedom of two sites. Strictly proved exact results in continuum percolation are limited to one dimension, but there are exact results valid in specific limits for higher-dimensional problems as well. Both types of exact results can be traced back to treelike structures; however, those trees have fundamentally different origins.

The central observable in continuum percolation is the pair connectedness $P(\boldsymbol{r}_1, \boldsymbol{r}_2)$, which in analogy to the total correlation function in liquid state theory satisfies an Ornstein-Zernike type equation,

$$P(\boldsymbol{r}_1, \boldsymbol{r}_2) = C^\dagger(\boldsymbol{r}_1, \boldsymbol{r}_2) + \int d\boldsymbol{r}_3\, \rho(\boldsymbol{r}_3) C^\dagger(\boldsymbol{r}_1, \boldsymbol{r}_3) P(\boldsymbol{r}_3, \boldsymbol{r}_2), \tag{36}$$

with the direct connectedness $C(\boldsymbol{r}_1, \boldsymbol{r}_2)$ and the one-particle density ρ [20]. The pair connectedness is defined so that $P(\boldsymbol{r}_1, \boldsymbol{r}_2) d\boldsymbol{r}_1 d\boldsymbol{r}_2$ describes the probability of finding two particles in the respective volume elements $d\boldsymbol{r}_1$ and $d\boldsymbol{r}_2$, which are also part of the same connected component. Typically, particles are considered connected according to a short range connectivity criterion. The partition sum can be expanded in Mayer f bonds,

$$f(\boldsymbol{r_1}, \boldsymbol{r_2}) = \exp[-\beta V(\boldsymbol{r_1}, \boldsymbol{r_2})] - 1, \tag{37}$$

with the thermal energy scale $\beta = (k_B T)^{-1}$ and the potential V of the pair interaction between particles. The connectivity Mayer $f^\dagger$ bond

$$f^\dagger(\boldsymbol{r_1}, \boldsymbol{r_2}) = \begin{cases} \exp[-\beta V(\boldsymbol{r_1}, \boldsymbol{r_2})] & \text{if 1 and 2 are connected,} \\ 0 & \text{otherwise,} \end{cases} \tag{38}$$

and f^* bond ($f^* \equiv f - f^\dagger$) additionally distinguish between connected and unconnected pairs of particles. The density expansion of the pair connectedness features integrals over $f^\dagger$ and f^* which represent the cluster structure of a cluster connecting $\boldsymbol{r_1}$ to $\boldsymbol{r_2}$. On a tree the connection between two particles at $\boldsymbol{r_1}$ and $\boldsymbol{r_2}$ can be established in only one way; hence, the only terms remaining in the expansion of P are chains of $f^\dagger$ bonds. Those chains are conveniently generated by the integral equation (36) with $C^\dagger \equiv f^\dagger$, a closure relation which is commonly referred to as the second virial approximation. Clearly, this approximation neglects any kind of thermal correlation between three or more bodies. Nevertheless, as it contains the leading order term in a density expansion, the approximation becomes viable in the low density limit. Consequently, the second virial approximation performs well if the critical density is low because higher order thermal correlations are suppressed. So an effectively treelike structure can be induced by the specific interaction. The perhaps most notable example of such a system is hard spherocylinders in three dimensions. As the aspect ratio becomes large, the percolation threshold goes to zero. Since the virial coefficients maintain their order of magnitude, the second virial approximation becomes exact at the percolation threshold in the Onsager limit of infinitely long and thin rods [8,37]. Conversely, for two-dimensional overlapping line segments the second virial approximation fails as the critical density, $\rho_c \approx 5.63$ particles per line segment length squared, is large and clusters in the barely subcritical regime are far from treelike [38].

Another example of asymptotic exactness is the percolation of fully penetrable hyperspheres in high-dimensional spaces. The critical density of hyperspheres becomes smaller as the dimension is increased, so that ultimately, the probability of more than two spheres meeting becomes negligible. In this case, the tree is generated purely by entropy. Clearly, the only truly exact results are those of the associated limit, hence featuring a vanishing percolation threshold.

Notice that the percolation threshold is computed from Eq. (36) as the divergence of the mean cluster size. For the simplest case of radial symmetry, the convolution can be resolved by Fourier transform, and the critical density satisfies

$$\rho \lim_{\boldsymbol{k}\to\boldsymbol{0}} C^\dagger(\boldsymbol{k}) = \rho \int d\boldsymbol{r}\, C^\dagger(\boldsymbol{r}) = 1. \tag{39}$$

For a system without interaction, e.g., fully penetrable spheres, the integral in (39) in the second virial approximation, $C^\dagger \equiv f^\dagger$, is simply the connected volume of a single particle. Thus, Eq. (39) means percolation requires a particle to have one neighbor on average, which is the notion that led us to all the exact solutions before. This remains true for interacting but very dilute systems as long as the total correlation function is approximated well by the Mayer f bond. Importantly, the accuracy breaks down beyond the low density limit, so the structure of the percolating network cannot be expected to be accurately depicted by the second virial approximation.

The only systems in continuum percolation allowing for a complete solution that is exact at all densities are one-dimensional; see [39] for a comprehensive overview. For one-dimensional systems with a short range connectivity criterion, the line topology imposes a global ordering. A connection to a distant particle requires a connection to its nearest neighbor in that direction. Given nearest-neighbor interactions, a connecting path is built as a chain of mutually independent nearest neighbors. Knowing the density distribution of the nearest neighbor, we can compute the pair-connectedness functions P exactly. This leads to the only exactly known pair-connectedness functions for ideal and hard line segments. The percolation threshold in these cases, however, is infinity. Accordingly, all exactly known percolation

thresholds in continuum percolation are trivial. This concludes our overview of the range of exactly solved percolation problems which all, in one way or another, contain a treelike structure. For all other problems we need to resort to approximations or brute force computational techniques. However, the exact solutions derived by duality have inspired the most accurate simulation techniques for a two-dimensional system. Since the concept of an average activity is easily generalized to three dimensions, the surface activity in an artificial hierarchy provides an interesting observable in a simulation. This, however, shall be discussed elsewhere.

IV. CONCLUSION

We have presented an overview of and a perspective on exactly solved percolation problems, illustrating that all these problems share the property of treelikeness. The treelike structure can be a matter of perspective (random graphs), an "accidental" cancellation of loops (two-dimensional lattices), or thermodynamically imposed (continuum percolation). As a consequence, we proposed a simple percolation criterion based on the Bethe lattice which correctly predicts the percolation thresholds of those systems. In addition, we generalized the relationship between known bond and site percolation problems and found classes of exactly solvable site-bond percolation models. Finally, we were able to extend the duality-inspired solutions to nonperiodic lattices and devised a method of generating a planar lattice with an arbitrary prescribed percolation threshold.

ACKNOWLEDGMENT

We acknowledge funding by the German Research Foundation under Project No. 404913146.

[1] S. R. Broadbent and J. M. Hammersley, Math. Proc. Cambridge Philos. Soc. **53**, 629 (1957).
[2] D. Stauffer and A. Aharony, *Introduction to Percolation Theory* (CRC Press, Boca Raton, FL, 2018).
[3] G. Grimmett, *Percolation* (Springer, New York, 1999).
[4] C. Moore and M. E. J. Newman, Phys. Rev. E **61**, 5678 (2000).
[5] B. Karrer and M. E. J. Newman, Phys. Rev. E **82**, 016101 (2010).
[6] M. Li, R.-R. Liu, L. Lü, M.-B. Hu, S. Xu, and Y.-C. Zhang, Phys. Rep. **907**, 1 (2021).
[7] A. Hunt, R. Ewing, and B. Ghanbarian, *Percolation Theory for Flow in Porous Media*, Lecture Notes in Physics (Springer, Switzerland, 2014), Vol. 880.
[8] A. V. Kyrylyuk and P. van der Schoot, Proc. Natl. Acad. Sci. USA **105**, 8221 (2008).
[9] F. Coupette, L. Zhang, B. Kuttich, A. Chumakov, S. V. Roth, L. González-García, T. Kraus, and T. Schilling, J. Chem. Phys. **155**, 124902 (2021).
[10] N. Araújo, P. Grassberger, B. Kahng, K. Schrenk, and R. M. Ziff, Eur. Phys. J.: Spec. Top. **223**, 2307 (2014).
[11] A. A. Saberi, Phys. Rep. **578**, 1 (2015).
[12] S. Smirnov and W. Werner, arXiv:math/0109120.
[13] J. Cardy, Ann. Phys. (NY) **318**, 81 (2005).
[14] H. Kesten, Commun. Math. Phys. **74**, 41 (1980).
[15] T. Vicsek and J. Kertesz, J. Phys. A **14**, L31 (1981).
[16] R. M. Ziff and B. Sapoval, J. Phys. A **19**, L1169 (1986).
[17] M. E. J. Newman and R. M. Ziff, Phys. Rev. E **64**, 016706 (2001).
[18] C. R. Scullard and J. L. Jacobsen, J. Phys. A **45**, 494004 (2012).
[19] M. Aizenman and D. J. Barsky, Commun. Math. Phys. **108**, 489 (1987).
[20] A. Coniglio, U. De Angelis, and A. Forlani, J. Phys. A **10**, 1123 (1977).
[21] M. E. Fisher and J. W. Essam, J. Math. Phys. **2**, 609 (1961).
[22] L. S. Schulman, J. Phys. A **16**, L639 (1983).
[23] P. Erdős and A. Rényi, Publ. Math. Inst. Hung. Acad. Sci. **5**, 17 (1960).
[24] B. Bollobàs, *Random Graphs* (Cambridge University Press, Cambridge, 2001).
[25] C. R. Scullard, Phys. Rev. E **73**, 016107 (2006).
[26] R. M. Ziff and C. R. Scullard, J. Phys. A **39**, 15083 (2006).
[27] C. Ding, Z. Fu, W. Guo, and F. Y. Wu, Phys. Rev. E **81**, 061111 (2010).
[28] A. Haji-Akbari and R. M. Ziff, Phys. Rev. E **79**, 021118 (2009).
[29] R. A. Neher, K. Mecke, and H. Wagner, J. Stat. Mech. (2008) P01011.
[30] W. Xu, J. Wang, H. Hu, and Y. Deng, Phys. Rev. E **103**, 022127 (2021).
[31] D. J. Barsky, G. R. Grimmett, and C. M. Newman, Probab. Theory Relat. Fields **90**, 111 (1991).
[32] C. R. Scullard and R. M. Ziff, J. Stat. Mech. (2010) P03021.
[33] M. F. Sykes and J. Essam, Phys. Rev. Lett. **10**, 3 (1963).
[34] R. M. Ziff, C. R. Scullard, J. C. Wierman, and M. R. Sedlock, J. Phys. A **45**, 494005 (2012).
[35] I. Kondor, J. Phys. C **13**, L531 (1980).
[36] M. Yanuka and R. Englman, J. Phys. A **23**, L339 (1990).
[37] A. L. R. Bug, S. A. Safran, and I. Webman, Phys. Rev. Lett. **54**, 1412 (1985).
[38] F. Coupette, R. de Bruijn, P. Bult, S. Finner, M. A. Miller, P. van der Schoot, and T. Schilling, Phys. Rev. E **103**, 042115 (2021).
[39] F. Coupette, A. Härtel, and T. Schilling, Phys. Rev. E **101**, 062126 (2020).